On-line Performance Assessment Method for a Model-Based Prognostic Approach

Yang Hu[1], Piero Baraldi[1], Francesco Di Maio[1], Enrico Zio[1,2,*]

[1] *Politecnico di Milano, Department of Energy, via Ponzio 34/3, Milan, 20133, Italy*

[2]*Chair on Systems Science and the Energetic challenge, European Foundation for New Energy-Electricite' de France, Ecole Centrale Paris and Supelec, Paris, France*

ABSTRACT

In this work, we propose a method for the on-line assessment of the performance of a prognostic approach in situation when degradation trajectories of other similar components are not available for traditional off-line performance assessment. The proposed method is applied on a prognostic approach based on a Particle Filter and Optimized Tuning Kernel Smoothing (PF-OTKS), extended to deal with situations characterized by scarce knowledge on the degradation process. A case study regarding the degradation of turbine blades is considered.

Key words: On-line Prognostics Performance Assessment; Model-based Prognostics; Particle Filter; Kernel Smoothing, Turbine Blade Creeping

1. INTRODUCTION

Model-based prognostic approaches can provide superior performances than data-driven approaches in situations characterized by the availability of reliable and accurate degradation models [1–5]. The decision maker needs to know the prognostic model performance to decide how confident he/she can be on the provided Remaining Useful Life (RUL) predictions. For this reason, classical metrics for off-line assessing the performance of a prognostic model, e.g. prognostic horizon, α-γ performance, relative accuracy and convergence, have been introduced [6–8]. Typically, these metrics require the knowledge of the true failure times of a population of components of the same type of the one which the prognostic model is intended to be applied to, which means that historical run-to-failure data must be available to perform (off-line) the prognostic model performance assessment. In practical engineering applications, the decision maker is more interested in the on-line prognostics performance of its component during operation, than in an 'average' population-based, off-line performance assessment.

The main objective of the present work is to propose a method for the on-line assessment of the performance of a model-based prognostic approach, using only information taken from the current degradation trajectory. The on-line performance assessment method proposed is based on a moving time window of past degradation measurements, on which the prognostics accuracy and precision are verified. Notice that the idea of using past degradation measurements to assess the reliability of prognostic predictions has been already considered in [9] in the different context of increasing the performance of the prognostic method. Here, new metrics are considered and adapted to the problem of assessing the performance of the prognostic model.

The prognostic approach considered in this paper is based on the use of a Particle Filter (PF) and Optimized Tuning Kernel Smoothing (OTKS) for jointly estimating the unknown parameters of the degradation model and the component RUL [9,10]. PF-based approaches to prognostics have been investigated by many researchers [4,12–16]. With respect to traditional Kalman-filter-based approaches [17–19], PF can be applied when the degradation model is non-linear, with non-additive and non-Gaussian process and measurement noises. For the setting of the prognostic approach, three cases are considered, characterized by different levels of knowledge on the degradation process:

Case 1: the degradation model is known, but the true values of some of its parameters are unknown [10,11];

Case 2: the effects of some operational/external conditions on the degradation process are unknown (degradation model partially unknown);

Case 3: the functional form of the evolution of the degradation process itself is unknown.

Further novelty of the present work is the adaptation of the PF-OTKS to deal with cases 2 and 3 above.

The on-line performance assessment method is verified with respect to a numerical case study concerning the prediction of the RUL of turbine blades degrading due to creeping.

The remainder of this paper is as follows: Section 2 illustrates the problem addressed in this work; the PF-OTKS algorithm and the on-line prognostic assessment approach are presented in Sections 3 and 4, respectively; Section 5 shows the application to the case study regarding the degradation of turbine blades; finally, Section 6 concludes the paper.

2. PROGNOSTIC PROBLEM SETTING

In this work, we consider a prognostic problem characterized by the unavailability of *i*) an accurate model of the degradation process of the component of interest and *ii*) observations of the degradation of similar components. More precisely, we assume that the only available degradation measurements $z_t(t = 1,2,\dots,t_p)$ come from the component of interest itself, i.e. the one for which we want to predict the RUL, from the beginning of its life (t=1) to the present time ($t = t_p$). The relation between the measurement z_t of a generic time t and the component degradation state, x_t, is described by the observation equation:

$$z_t = h(x_t, \upsilon_t) \tag{2.1}$$

where h is a possibly nonlinear function and υ_t is an i.i.d. random noise representing the measurement uncertainty. We assume that the generic model of the component degradation process is given by:

$$x_{t+1} = f\left(x_t, \mathbf{P}_t, \mathbf{e}_t, t, \boldsymbol{\omega}_t\right) \tag{2.2}$$

where f is a possibly non-linear function, $\mathbf{P}_t$ is the vector of model parameters values at time t, $\mathbf{e}_t$ is the vector that represents the external/operational conditions which influence the degradation process and $\boldsymbol{\omega}_t$ is an i.i.d. random process noise possibly non Gaussian, at time t.

We further assume that the function f can be decomposed into the product of two functions following the approach proposed in [20], where the influence of the external conditions on the component failure rates are represented by multiplicative factors:

$$x_{t+1} = f_0\left(x_t, \mathbf{P}_t, t, \omega_t^f\right) \cdot g\left(\mathbf{e}_t, \boldsymbol{\omega}_t^g\right) \tag{2.3}$$

where f_0 describes the degradation behavior in normal conditions and g represents the influence of the external conditions on the degradation process.

With respect to the knowledge available on these two functions, we consider three different cases characterized by decreasing knowledge available:

- Case 1

Functions f_0 and g are known, but the exact values of some parameters in vector **P** are unknown. This situation may occur, for example, when the main mechanisms governing the degradation process are known, but minor differences exist in the material and design of the component of interest, so that the model parameters values are different.

- Case 2

Function g is unknown. This situation describes a case in which the effects of the operational/external conditions on the degradation process are unknown. This situation is typically encountered when the degradation process has been mainly investigated by performing laboratory tests in controlled environment and operational conditions, but limited experience on the component degradation process in real operational and environmental conditions is available.

- Case 3

This is the extreme case in which one only knows that the degradation state, x, is increasing as time passes. It corresponds to situations in which the knowledge on the degradation process is so little that it is impossible to define models f_0 and g.

In all the three cases, we assume that the exact value of the failure threshold, Th, i.e., the maximum degradation state beyond which the system loses its function, is known.

Considering, for example, the degradation process of a Lithium battery, an indicator of the battery degradation is its capacity [21], whose time evolution is typically represented by using a double exponential law [22,23]. As batteries are built using different materials such as Li-MnO_2, Li-FeS_2, Li-Ag_2CrO_4, the true values of the model parameters maybe unknown (case 1). Further, the external/operational conditions in which the battery are used, such as temperature, humidity, charging and discharging currents, can influence the degradation process and the battery lifetime [22]. As the influences of the external/operational conditions are not explicitly taken into account by the double exponential model, the modeling of the car battery degradation corresponds to case 2 (degradation model only partially known). Finally, case 3 can be encountered in this example, considering a completely new battery design for special applications, e.g. graphene or titanium dioxide batteries: for these batteries, the applicability of the double exponential model may even be questionable.

3. THE PARTICLE FILTER AND OPTIMIZED TUNING KERNEL SMOOTHING - BASED PROGNOSTIC APPROACH

In order to cope with the prognostic problem setting outlined in the previous Section, we resort to an approach based on the use of PF-OTKS, which has been already applied with success to a prognostic problem characterized by unknown degradation model parameters (case 1) in [11]. In the present work, the approach is extended to deal with cases 2 and 3. Sections 3.1 and 3.2 briefly recall the basic ideas of the PF-Based prognostics approach and of PF-OTKS, whereas Sections 3.3 and 3.4 outline the PF-OTKS extension to the new situations of cases 2 and 3, respectively.

3.1. Particle Filter-Based Prognostics

The PF-based approach to prognostics can be divided into two steps [24–27]:

(1) A filtering step, whose objective is to estimate the component degradation state at the present time, t_p, using the available on-line measurements $z_t(t = 1,2,\dots,t_p)$.

(2) A prediction step, whose objective is the prediction of the component RUL using the degradation state estimated in step (1).

With respect to step (1), the main idea of PF is to estimate the posterior Probability Density Function (PDF) of the degradation state, x_t at a generic time *t*, using weighted particles $\{x_t^i, w_t^i\}$:

$$p_e(x_t|z_{1:t}) \approx \sum_{i=1}^{N} w_t^i \delta\left(x_t - x_t^i\right) \tag{3.1}$$

where $p_e(x_t|z_{1:t})$ is the estimated posterior PDF of x_t, $z_{1:t}$ is the vector of available measurements of the degradation state from time 1 to *t*, δ is the Dirac Delta function, $x_t^i(i = 1,2,\dots,N)$ are the particles sampled from the importance sampling PDF, $q(x_t|\mathbf{z}_{1:t})$, and w_t^i is the weight assigned to particle x_t^i. By setting $q(x_t|\mathbf{z}_{1:t}) = p_f(x_t|x_{t-1})$, where $p_f(x_t|x_{t-1})$ is the predicted PDF obtained from equation (2.3), the equation for weight updating, once a new measurement $\mathbf{z}_t$ becomes available, is:

$$w_t'^i = w_{t-1}'^i p\left(z_t|x_t^i\right);\ w_t^i = \frac{w_t'^i}{\sum_{i=1}^{N} w_t'^i} \tag{3.2}$$

where $p(\mathbf{z}_t|x_t^i)$ is the likelihood of $\mathbf{z}_t$ given the particle x_t^i, which can be derived from the measurement equation (2.1). The interested reader can refer to [24,27] for a detailed description of PF for degradation state estimation.

After the degradation state has been estimated, we can use equation (2.3) to predict the future degradation trajectory. The RUL prediction can be found by simulating the particle evolutions until they reach the failure threshold *Th*. The RUL associated to the *i*-th particle at time *t* is given by [9,28]:

$$RUL_t^i = \left\{\left(T_t^i - 1 - t\right)\middle| x_{T_t^i - 1} < Th,\ x_{T_t^i} \geq Th\right\} \tag{3.3}$$

where T_t^i, which is the first time the particle reaches the threshold *Th*, can be computed by iteratively applying equation (2.3). Thus, the PDF of RUL and its expected value are given by:

$$\begin{aligned} p_f(RUL|z_{1:t}, Th) &\approx \sum_{i=1}^{N} w_t^i \delta(RUL - RUL_t^i) \\ \hat{RUL}_t &= \sum_{i=1}^{N} w_t^i \cdot RUL_t^i \end{aligned} \tag{3.4}$$

3.2. The PF-OTKS approach in case 1

The combined estimate of the equipment degradation state and degradation model parameters can be performed by using an extended PF approach [11,29]. The idea is to consider the model parameters as elements of the state vector which is estimated by PF. Thus, the generic augmented *i*-th particle, k_t^i, is extended as $\{x_t^i, \mathbf{P}_t^i, w_t^i\}$, where x_t^i represents the degradation state (particle), $\mathbf{P}_t^i$ the model parameters at time *t* and w_t^i is the weight associated to the particle x_t^i. Thus, equation (2.3) becomes a system of two equations, one describing the transition of the degradation state (f) and the other the evolution of the parameters (f_p):

$$\begin{aligned} x_{t+1}^i &= f_0\left(x_t^i, \mathbf{p}_t^i, t, \omega_t^f\right) \cdot g\left(\mathbf{e}_t, \omega_t^g\right) \\ \mathbf{p}_{t+1}^i &= f_p(\mathbf{p}_t^i) \end{aligned} \tag{3.5}$$

With respect to the definition of f_p, there are different options. In some works [13,14,21], the equation describing the parameter evolution is:

$$\mathbf{p}_{t+1}^i = g_2(\mathbf{p}_t^i) = \mathbf{p}_t^i + N(0, \sigma_{AN}^2) \tag{3.6}$$

where σ_{AN}^2 is the variance of the artificial noise. Notice, however, that this method cannot be applied to our prognostic problem since it requires a priori setting of the value of σ_{AN}^2, which is difficult to achieve by trial and error attempts, due to the unavailability of complete examples of degradation trajectories in similar components. In order to overtake these difficulties, we consider an alternative PF approach based on a Kernel Smoothing (KS) algorithm developed by the authors and whose details are described in [10]. Kernel smoothing consists in the application of two different procedures to the population of particles: shrinkage and perturbation. Shrinkage aims at reducing the variability in the particle population by moving the single particle $\mathbf{p}_t^i$ towards the current estimated values $\hat{\mathbf{p}}_t$, whereas perturbation adds a controlled noise on $\mathbf{p}_t^i$ after the shrinkage in order to maintain the desired variance in the population [30–32]. The application of this algorithm requires the a-priori setting of the smoothing parameter which determines the amplitude of the particle shrinkage. Too large value of this parameter can cause an extra shrinkage and perturbation of the particles, which will result in a bias of the model parameter estimates. On the other side, too small values of the shrinkage parameter can result in the impoverishment of the population of particles. Thus, the proper setting of the smoothing parameter is a critical issue in the cases addressed in this work, where historical trajectories describing the component degradation from the beginning of its life until failure are unavailable and, thus, a trial and error approach cannot be followed. In order to overtake this difficulty, in this work we adopt the scheme proposed in [29] for setting the

proper value of the smoothing parameter, based on the minimization of the Kullback–Leibler (KL) divergence between the predicted and posterior PDFs. Since this method employs only the information provided by on-line degradation measurements, it can be effectively applied to the problem setting here considered. The readers interested on more details of the PF-OTKS approach can refer to [11] and Appendix 1.

3.3. PF-OTKS in case 2

In case 2, function g in equation (2.3) is completely unknown. Our approach to deal with this situation is based on the substitution of function $g\left(\mathbf{e}_t, \boldsymbol{\omega}_t^g\right)$ with a random noise, λ_t, distributed according to a given distribution $\lambda_t \sim \mathrm{Y}(\mathbf{L}_t)$, where $\mathrm{Y}(\mathbf{L}_t)$ is a statistical distribution with unknown parameters $\mathbf{L}_t$. Thus, equation (2.3) becomes:

$$x_{t+1} = f_0\left(x_t, \mathbf{P}_t, t, \boldsymbol{\omega}_t\right) \cdot \lambda_t . \tag{3.7}$$

Then, PF-OTKS can be used to deal with the problem of jointly estimating the component degradation state and the parameters $\mathbf{L}_t$ of the probability distribution $\mathrm{Y}(\mathbf{L}_t)$. In practice, in this case, the extended particle is defined by $k_t^i = \{x_t^i, \mathbf{L}_t^i, w_t^i\}$, and the same procedure illustrated in the previous Section 3.2 can be applied for the joint estimation of the component RUL and the parameters $\mathbf{L}_t$, some execution procedures can be found in Appendix 2. This approach is based on the assumption that the parameters $\mathbf{L}_t$ do not change as time passes. This is verified for those applications in which the effects of the external conditions on the degradation process are not influenced by the current degradation level. Furthermore, since the noise λ_t does not depend on the external conditions e, we also assume that the external conditions are following a stochastic distribution which is not changing as time passes. Future research will be devoted to the investigation of the possibility of relaxing these assumptions.

3.4. PF-OTKS in case 3

In the case in which both functions f_0 and g are unknown, a possibility is to substitute equation (2.3) with:

$$x_{t+1} = x_t + \beta_t \tag{3.8}$$

where β_t is a random noise used to replace the whole degradation model. Similarly to what done in Section 3.3 to deal with case 2, also in this case we assume that $\beta_t \sim \mathrm{Y}(\mathbf{L}_t)$, where $\mathrm{Y}(\mathbf{L}_t)$ is characterized by the unknown parameters $\mathbf{L}_t$. Then, assuming that the parameters $\mathbf{L}_t$ are time independent, they can be estimated jointly to the degradation state by adopting PF-OTKS. Notice that equation (3.8) can be applied only to degradation processes for which the probability distribution of the degradation increment, $x_{t+1} - x_t$, between two consecutive time instants, t and t+1, does not depend on the age of the component, t. Future research work will be devoted to the investigation of the possibility of relaxing this hypothesis by substituting equation (3.8) with

$$x_{t+1} = a_0 + a_1 x_t + a_2 x_t^2 + \ldots + a_n x_t^n + \beta_t \tag{3.9}$$

where a_i, i=1,…,n are unknown coefficients whose values are to be estimated by the PF-OTKS.

4. ON-LINE ASSESSMENT OF THE PROGNOSTIC MODEL PERFORMANCE

Traditional prognostic metrics assess the general validity of a prognostic model. They typically require the availability of several degradation trajectories, from the beginning of the degradation process to the failure, and they off-line measure the average performance of the prognostic model on these trajectories, using the known failure times. Since the prognostic problem here addressed is characterized by the unavailability of complete degradation trajectories (as is often the case in practice), the assessment of the prognostic model performance requires the definition of new metrics. Furthermore, in practice we are not really interested in assessing the average performance of the model, but rather its performance with respect to the particular degradation trajectory that is being followed.

The performance assessment method here proposed requires the availability of i) the measurement $z_{1:t_p}$, collected from the onset of the degradation trajectory until the present time t_p on the degrading component of interest and ii) a generic model-based prognostic approach based on the use of a Bayesian filter. Thus, the applicability of the performance assessment method is not limited to the PF-OTKS approach of Section 3, but can be extended to Kalman Filters, Extended Kalman Filters, PFs and other Bayesian approaches.

The basic idea behind the on-line performance assessment method is to verify whether the predictions of the degradation state provided in the past have been accurate and precise. In particular, we consider past predictions of the degradation state on time horizons similar to the RUL predicted at the present time, $\widehat{RUL}_{t_p}$.

The method is based on the following steps:

(1) At the present time t_p, we fix a time window length equal to the present RUL prediction, $\widehat{RUL}_{t_p}$;

(2) From a time t^*, at which we can assume that the prognostic model is sufficiently stable, i.e. the estimates of the model parameters are not significantly varying, we build the time windows $win_t = [t, t + \widehat{RUL}_{t_p}]$ with $t = t^*, t^* + 1, \dots, t_p - \widehat{RUL}_{t_p}$ (Figure 1). Notice that the total number of time windows which can be built is $t_p - \widehat{RUL}_{t_p} - t^* + 1$.

Although we do not know the true component degradation state, x_t, at time *t*, we can estimate it using all the knowledge available at the present time, t_p. In particular, the best possible estimate of the degradation state of the component at the end of the time window, $x_{t+\widehat{RUL}_{t_p}}$, is given by the posterior PDF, $p_e\left(x_{t+\widehat{RUL}_{t_p}} \middle| z_{1:t_p}\right)$, which can be obtained by the PF-based prognostic model using all the available measurement $z_1, z_2, \dots, z_t, \dots, z_{t_p}$, including those collected after time *t*. To this aim, according to [25], we can apply:

$$p_e\left(x_{t+\widehat{RUL}_{t_p}} \middle| z_{1:t_p}\right) \approx \sum_{i=1}^{N} w_{t_p}^i \delta\left(x_t^i - x_t\right) \tag{4.1}$$

where $w_{t_p}^i$ is the weight of particle i computed at time t_p, Then, $\hat{x}_{t+R\hat{U}L_{t_p}|z_{1:t_p}}$, i.e. the estimate of the degradation state at the end of the time window, $t + R\hat{U}L_{t_p}$, is given by:

$$\hat{x}_{t+R\hat{U}L_{t_p}|z_{1t_p}} = \sum_{i=1}^{N} w_{t_p}^i x_t^i \tag{4.2}$$

The next step (3) of the procedure is applied to each time window, $win_t = [t, t + R\hat{U}L_{t_p}]$ with $t = t^*, t^* + 1, \dots, t_p - R\hat{U}L_{t_p}$.

(3) In order to verify the performance of the method on time window win_t, we compare the estimate of the PDF of the degradation state predicted at the beginning of the time window, $p_f\left(x_{t+R\hat{U}L_{t_p}}\middle|z_{1:t}\right)$, with the best available posterior PDF of the degradation state, obtained by using alll the available measurements, $z_{1:t_p}$, i.e. $p_e\left(x_{t+R\hat{U}L_{t_p}}\middle|z_{1:t_p}\right)$. This comparison can be performed by considering classical prognostic metrics. In particular, in this work, we consider accuracy, coverage and prediction interval lengths of the RUL; they are computed by:

a) Artificially assuming that the failure threshold is provided by the estimated value of the degradation at time $t + R\hat{U}L_{t_p}$, computed considering all the available information until the present time, i.e. $Th_t = \hat{x}_{t+R\hat{U}L_{t_p}|z_{1:t_p}}$. According to this assumption, the true RUL of the component at time t is exactly $R\hat{U}L_{t_p}$.

b) Estimating the PDF, $p_f(RUL_t|z_{1:t}, Th_t)$, of the RUL which is predicted at time t by the PF-based prognostic approach. This estimate is based on equation (3.4), assuming the degradation threshold Th_t. This PDF has to be compared to $R\hat{U}L_{t_p}$, i.e. the true RUL of the component assuming the same failure threshold.

c) Computing the metrics of interest for assessing the performance of the prognostic model in the time window win_t. In this work, we focus on accuracy, coverage and prediction interval lengths. The three metrics are defined by:

$$win_t.a = \int \left|RUL_t - R\hat{U}L_{t_p}\right| p_f\left(RUL_t|z_{1:t}, Th_t\right) d(RUL_t) \tag{4.3}$$

$$win_t.c = \begin{cases} 1 & C_{\inf}\left(p_f\left(RUL_t|z_{1:t}, Th_t\right)\right) < R\hat{U}L_{t_p} < C_{\sup}\left(p_f\left(RUL_t|z_{1:t}, Th_t\right)\right) \\ 0 & otherwise \end{cases} \tag{4.4}$$

$$win_t.w = C_{\sup}\left(p_f\left(RUL_t|z_{1:t}, Th_t\right)\right) - C_{\inf}\left(p_f\left(RUL_t|z_{1:t}, Th_t\right)\right) \tag{4.5}$$

where $C_{\inf}\left(p_f\left(RUL_t|z_{1:t}, Th_t\right)\right)$ and $C_{\sup}\left(p_f\left(RUL_t|z_{1:t}, Th_t\right)\right)$ are the upper and lower bounds of the 90% prediction interval of the $p_f\left(RUL_t|z_{1:t}, Th_t\right)$.

(4) Compute the average of the accuracy, coverage and width of the prediction interval in all the time windows win_t, $t = t^*, t^* + 1, \dots, t_p - R\hat{U}L_{t_p}$:

$$RMSE_{t_p} = \sqrt{\frac{\sum_{t=t^*}^{t_p - t^* - R\hat{U}L_{t_p}+1} win_t.a^2}{t_p - t^* - R\hat{U}L_{t_p}+1}} \tag{4.6}$$

$$CR_{t_p} = \frac{1}{t_p - t^* - R\hat{U}L_{t_p}+1} \sum_{t=t^*}^{t_p - t^* - R\hat{U}L_{t_p}+1} win_t.c \tag{4.7}$$

$$width_{t_p} = \frac{1}{t_p - t^* - R\hat{U}L_{t_p}+1} \sum_{t=t^*}^{t_p - t^* - R\hat{U}L_{t_p}+1} win_t.w \tag{4.8}$$

where $RMSE_{t_p}$, CR_{t_p} and $width_{t_p}$ are the obtained Root Mean Square Error, Coverage Rate and average width over all the considered time windows. Small values of $RMSE_{t_p}$ indicate that the expected prediction error at t_p is small and, thus, that the model is providing accurate predictions. High value of CR_{t_p} means that the prediction interval has high probability to cover the true value $R\hat{U}L_{t_p}$ and, thus, the representation of the uncertainty on the RUL prediction is satisfactory. Small $width_{t_p}$ indicates that the prediction is precise. Generally, good prognostics model are associated with CR_{t_p} values around 90%, while $RMSE_{t_p}$ and $width_{t_p}$ should be as small as possible.

Figure 1 Sketch of moving time window approach

Table 1 Time window attributes

Notice that the application of the proposed on-line performance assessment method to the PF-OTKS algorithm is based on the hypothesis that all the parameters in the degradation models (namely $\mathbf{P}_t$ in equation (2.3) or $\mathbf{L}_t$ in equation (3.7) and (3.8)) are stationary.

5. NUMERICAL APPLICATION

In this Section, the prognostic approach and the on-line performance assessment method presented in Sections 3 and 4, respectively, are verified with respect to a numerical application regarding the RUL prediction of a turbine blade undergoing degradation [33–36]. The degradation mechanism that we consider is a creep deformation which can lead to the loss of the blade, i.e. one of the most feared failure modes in turbines [36]. Creep is an irreversible deformation process affecting materials exposed to a load below the elastic limit for a protracted length of time and at high temperature.

An indicator of the blade degradation at time, *t*, is the creep strain, ε_t. In this work, we simulate the creep evolution using the Norton Law [35, 36] and assuming that the dependence of the degradation from the temperature follows the Arrhenius law [39]. In practice, we iteratively apply:

$$\varepsilon_{t+1} = \varepsilon_t + A \cdot \exp\left(-\frac{Q}{RT_t}\right)\left(K\omega_t^2 + \gamma_t\right)^n \cdot \Delta t$$
$$T_t = T_0 + \triangle T, \omega_t = \omega_0 + \triangle \omega \tag{5.1}$$

where Q is the activation energy, R is the ideal gas constant, T_t is the blade operating temperature at time t, ω_t is the turbine rotational speed, K is a constant related to the material density and turbine radius, Δt is the time step used for the discretization of the differential equation, and A and n are material-inherent parameters. The parameters and process noise setting used to perform the simulation are taken from [26, 38] and reported in Table 2. Notice that the randomness of the degradation process is represented by:

- the process noise, γ_t, which is used to model the fluctuation of the blade stress during operation. The uncertainty is mainly caused by fabrication defects, aging and corrosion of the blade, vibrations of the equipment or turbulences of the gas flow.
- the random variations, ΔT and $\Delta\omega$ of the external conditions around their mean values, T_0 and ω_0, respectively.

Table 3 reports the parameters of the Gaussian distributions used to model the uncertainty on the external conditions, γ_t, ΔT and $\Delta\omega$. With respect to γ_t, two different settings are considered in order to represent a situation characterized by small uncertainty on the blade stress (standard deviation equal to 10) and another by high uncertainty (standard deviation equal to 30).

Table 2 Parameters of the degradation model

Table 3 Parameters of the distributions representing the process noises

In both uncertainty settings, a degradation trajectory has been simulated, made by 750 simulated elongations, $\varepsilon_1, \varepsilon_1, \ldots, \varepsilon_{750}$, where 750 has been chosen in order to guarantee that the trajectories reach the failure threshold. Then, the corresponding creep strain measurements, M_t, have been simulated using:

$$M_t = \varepsilon_t + N(0, \eta) \tag{5.2}$$

where $N(0, \eta)$ describes the measurement noise, with standard deviation $\eta = 0.01$ according to [40]. The time gap between two measurements is 5 days and the last measurement is performed at day 646. Figure 2 shows the two simulated degradation trajectories. Notice that the trajectory obtained considering large uncertainty on the blade stress is noisier and characterized by a faster degradation process than the one with small uncertainty. This is due to the fact that the noise Gaussian term γ_t in equation (5.1) appears at the power of n and, thus, the expected value of the degradation increment is influenced by the variance of the noise. In order to have comparable lifetimes in the two numerical case studies, we have adopted different values of the failure threshold (last row of Table 4).

Figure 2. Two examples of simulated degradation trajectories in the small (left) and large (right) uncertainty settings of the process noise.

5.1. Case studies and prognostic approaches

According to Section 2, the performance of the proposed prognostic approaches has been verified assuming three different situations of available information:

- Case 1 - the degradation model in equation (5.1) is known, but the true values of the material-inherent parameters, *A* and *n*, are unknown. The prognostic approach is here based on the application of the PF-OTKS algorithm illustrated in Section 3.2.
- Case 2 - the influence of the stress on the degradation is unknown. Thus, instead of using the complete degradation model provided by (5.1), we describe the influence of the stress applied to the blade on the degradation by using a random noise. In other words, according to Section 3.3, the PF-OTKS employs the model:

$$\begin{aligned} \varepsilon_{t+1} &= \varepsilon_t + A \cdot \exp\left(-\frac{Q}{RT_t}\right) \lambda_t \cdot \Delta t \\ \lambda_t &\sim U\left(L_t, H_t\right) \end{aligned} \tag{5.3}$$

  where λ_t is a random noise represented by a uniform distribution with unknown lower and upper bounds, L_t and H_t, respectively. The main reason to use a uniform distribution is that, according to the principle of insufficient reasoning of Laplace [41], this is the best choice when the only available knowledge is the range of values of the unknown quantity, whereas no information is available on the shape of the probability distribution.

- Case 3 - Experts believe that the degradation process is linear but no mathematical equation describing the degradation process is available. The PF-OTKS method proposed in Section 3.4 is applied to this case, by assuming:

$$\begin{aligned} \varepsilon_{t+1} &= \varepsilon_t + \beta_t \cdot \Delta t \\ \beta_t &\sim U\left(L_t', H_t'\right) \end{aligned} \tag{5.4}$$

  where β_t is a random noise represented by a uniform distribution with unknown lower and upper bounds, L_t and H_t, respectively. Also in this case the choice of the uniform distribution is justified by the fact that we have no prior information on the shape of the probability distribution.

5.2. RUL prediction

The PF-OTKS methods of Sections 3.2, 3.3 and 3.4 have been applied to cases 1, 2 and 3, respectively. Table 4 reports the prior distributions used within the PF-OTKS approach for the estimate of the unknown parameters. The aim of this setting is to assess whether the PF-OTKS can work even if the prior PDFs of the parameters are uncertain and their true values (reported in Table 2) are located in the tail of the prior distributions. The PF-OTKS is applied considering a number of particles equal to 1000 in each case; this number has been chosen in view of a tradeoff between estimation accuracy and computational burden.

Table 4 Prior distributions of the uncertain parameters

Figures 3, 4 and 5 show the RUL predictions obtained on a test trajectory in the small and large uncertainty blade stress settings.

Figure 3 RUL prediction in Case 1.
Left: small uncertainty on the blade stress; right: large uncertainty on the blade stress

Figure 4 RUL prediction in Case 2.
Left: small uncertainty on the blade stress; right: large uncertainty on the blade stress

Figure 5 RUL prediction in Case 3.
Left: small uncertainty on the blade stress; right: large uncertainty on the blade stress

In case 1, once few measurements are collected, the PF-OTKS provides satisfactory RUL predictions. In case 2, the PF-OTKS needs more measurements to identify the parameters of the noise distribution used to model the effect of the stress on the degradation process and to start providing satisfactory RUL predictions. In case 3, especially in the situation of large uncertainty on the blade stress, the RUL prediction is less accurate due to the limited information available on the degradation model and the large uncertainty. As expected, all the predictions obtained considering large uncertainty on the blade stress are less accurate and characterized by larger prediction intervals than those obtained in the small uncertainty settings.

It is also interesting to observe that the fewer the information available on the degradation process (case 3), the smaller the prediction interval. This is due to the fact that in cases 2 and 3, the PF-OTKS tends to underestimate the variance of the process noises, as it is shown in Figure 6 which compares the probability distribution of the true degradation rate and that obtained by PF-OTKS considering large uncertainty on the blade stress. In case 1, a very satisfactory estimation of the degradation rate distribution is obtained, whereas in cases 2 and 3 the variance of the true distribution is underestimated and the PDF tail towards large values is not represented; this causes a small RUL coverage and an underestimation of the degradation state.

Figure 6 Probability Distribution Functions (PDFs) of degradation rate

5.3. On-line performance assessment

In this Section, we verify the proposed on-line performance assessment method. Figures 7, 8 and 9 show the three on-line assessment indicators of Section 4, RMSE, CR and average width of the prediction interval.

Figure 7 On-line RMSE.
Left: small uncertainty on the blade stress; right: large uncertainty on the blade stress

Figure 8 On-line CR.
Left: small uncertainty on the blade stress; right: large uncertainty on the blade stress

Figure 9 On-line average width of prediction interval.
Left: small uncertainty on the blade stress; right: large uncertainty on the blade stress

In order to guarantee that the parameter estimates provided by the PF-OTKS are stable and that there are enough time windows to calculate the prognostic metrics, we start applying the on-line performance assessment at $t = 445$.

With respect to the accuracy, Figure 7 shows that the estimated on-line RMSE is lower when the process noise is smaller and the information available is more (case 1). These results represent the real performance of the model on the developing degradation trajectory (Figure 3, Figure 4 and Figure 5). The estimated coverage rate is above 90% in all three cases with small process noise, whereas, in the simulation with large process noise, the coverage is satisfactory only in case 1 and in case 2 after $t = 500$. These results confirm the effectiveness of the on-line performance assessment since the real coverage provided by the method shown in Figures 3-5 is similar to the on-line estimated. Finally, with respect to the average widths of the prediction interval shown in Figure 9, the fact that in case 1 the interval is larger than in cases 2 and 3, characterized by less information, indicates that the process uncertainties are underestimated in cases 2 and 3.

In order to verify the correctness of the on-line assessment results, we have performed both an off-line and an on-line performance assessment for 50 new degradation trajectories which have been simulated using the parameters settings in Tables 2 and 3. Figures 10, 11 and 12 show the average values of RMSE, CR and width of the prediction interval, computed at 2 different time ($t_p = 451$ and 601), in the three cases of information available, considering both the small and large blade noise settings.

Figure 10 On-line and off-line RMSE
Left: small uncertainty on the blade stress; right: large uncertainty on the blade stress

Figure 11 On-line and off-line CR.
Left: small uncertainty on the blade stress; right: large uncertainty on the blade stress

Figure 12 On-line and off-line average width of prediction interval.
Left: small uncertainty on the blade stress; right: large uncertainty on the blade stress

The obtained results confirm that the on-line performance assessment method is able to estimate with a good precision the true performance of the prognostic method.

6. CONCLUSIONS

The prediction of the RUL of high-value and safety-critical components is very important for their safe and efficient operation. In this work, we have developed a new method for on-line assessing the

performance of prognostic models in predicting the evolution of developing degradation trajectories. The underlying idea is to verify whether past predictions provided by the degradation model are accurate and precise, as the degradation state measurements are collected in time.

The method has been illustrated considering the problem of RUL prediction by a model-based prognostic approach based on the PF-OTKS algorithm previously developed by the authors. Six numerical experiments regarding the degradation of a turbine blade have been performed, considering cases characterized by different levels of knowledge and uncertainty on the degradation process.

The original contributions of the work are:

- with regards to PF-OTKS, the extension of the method to treat cases of processes for which the functional dependence on external/operation conditions is unknown (case 2) or even the functional form of the evolution of the degradation process itself is unknown (case 3);
- with regards to the performance assessment, the development of a method that can be used on-line for assessing prognostics performance based solely on the developing degradation trajectory of interest.

The results have shown that PF-OTKS can provide satisfactory RUL predictions except, as expected, when the knowledge on the degradation process is very scarce and the process noise is large. Even in this case, the on-line performance assessment method has proved capable of providing reliable estimates of the prognostic model performance. Its use is, thus, very relevant for decision makers to decide whether the RUL prediction provided is reliable and can be used to plan for confident maintenance and operation decisions.

ACKNOWLEDGEMENT

Yang Hu gratefully acknowledges the financial support from China Scholarship Council and Politecnico di Milano (No. 201206110018). The participation of Enrico Zio to this research is partially supported by the China NSFC under grant number 71231001. The participation of Piero Baraldi and Francesco Di Maio is supported by the European Union Project INNovation through Human Factors in risk analysis and management (INNHF, www.innhf.eu) funded by the 7th framework program FP7-PEOPLE-2011-Initial Training Network: Marie-Curie Action.

REFERENCES

[1] Daigle M, Goebel K. Model-based prognostics under limited sensing. Aerospace Conference, 2010 IEEE, 2010, p. 1–12.

[2] Saha B, Goebel K. Modeling Li-ion Battery Capacity Depletion in a Particle Filtering Framework. Annual Conference of the Prognostics and Health Management Society, 2009, p. 1–10.

[3] Cadini F, Zio E, Avram D. Monte Carlo-based filtering for fatigue crack growth estimation. Probabilistic Engineering Mechanics 2009;24:367–73.

[4] An D, Kim NH, Choi J-H. Practical options for selecting data-driven or physics-based prognostics algorithms with reviews. Reliability Engineering & System Safety 2015;133:223–36.

[5] Shao X, Huang B, Lee JM. Constrained Bayesian state estimation - A comparative study and a new particle filter based approach. Journal of Process Control 2010;20:143–57.

[6] Saxena A, Celaya J, Balaban E, Goebel K, Saha B, Saha S, et al. Metrics for evaluating performance of prognostic techniques. 2008 International Conference on Prognostics and Health Management 2008.

[7] Saxena A, Celaya J, Saha B, Saha S, Goebel K. Metrics for Offline Evaluation of Prognostic Performance. International Journal of Prognostics and Health Management 2010:1–20.

[8] Saxena A, Sankararaman S, Goebel K. Performance Evaluation for Fleet-based and Unit-based Prognostic Methods n.d.:1–12.

[9] Zio E, Peloni G. Particle filtering prognostic estimation of the remaining useful life of nonlinear components. Reliability Engineering & System Safety 2011;96:403–9.

[10] Hu Y, Baraldi P, Di Maio F, Zio E. A particle filtering and kernel smoothing-based approach for new design component prognostics. Reliability Engineering & System Safety 2014;134:19–31.

[11] Hu Y, Baraldi P, Di Maio F, Zio E. A Prognostic Approach Based on Particle Filtering and Optimized Tuning Kernel Smoothing. second european conference of the prognostics and health management society, Nantes, France: 2014.

[12] Olivares BE, Cerda Muñoz MA, Orchard ME, Silva JF. Particle-Filtering-Based Prognosis Framework for Energy Storage Devices With a Statistical Characterization of State-of-Health Regeneration Phenomena. IEEE Transactions on Instrumentation and Measurement 2012:1–13.

[13] Orchard M, Tobar F, Vachtsevanos G. Outer feedback correction loops in particle filtering-based prognostic algorithms: Statistical performance comparison. Studies in Informatics and Control 2009;18:295–304.

[14] Daigle MJ, Goebel K. Model-Based Prognostics With Concurrent Damage Progression Processes. Ieee Transactions on Systems Man Cybernetics-Systems 2013;43:535–46.

[15] An D, Choi JH, Kim NH. Prognostics 101: A tutorial for particle filter-based prognostics algorithm using Matlab. Reliability Engineering & System Safety 2013;115:161–9.

[16] Prakash J, Patwardhan SC, Shah SL. On the choice of importance distributions for unconstrained and constrained state estimation using particle filter. Journal of Process Control 2011;21:3–16.

[17] Wan EA, Van der Merwe R. The unscented Kalman filter for nonlinear estimation. Adaptive Systems for Signal Processing, Communications, and Control Symposium 2000 AS-SPCC The IEEE 2000 2000:153–8.

[18] Van der Merwe R, Wan EA. The square-root unscented Kalman filter for state and parameter-estimation. Acoustics, Speech, and Signal Processing, 2001 Proceedings (ICASSP '01) 2001 IEEE International Conference on 2001;6:3461–4 vol.6.

[19] Julier SJ, Uhlmann JK. Unscented filtering and nonlinear estimation. Proceedings of the IEEE 2004;92:401–22.

[20] Handbook M. Reliability prediction of electronic component. MIL-HDBK-217F; n.d.

[21] He W, Williard N, Osterman M, Pecht M. Prognostics of lithium-ion batteries based on Dempster–Shafer theory and the Bayesian Monte Carlo method. Journal of Power Sources 2011;196:10314–21.

[22] Omar N, Monem MA, Firouz Y, Salminen J, Smekens J, Hegazy O, et al. Lithium iron phosphate based battery – Assessment of the aging parameters and development of cycle life model. Applied Energy 2014;113:1575–85.

[23] Zhang J, Lee J. A review on prognostics and health monitoring of Li-ion battery. Journal of Power Sources 2011;196:6007–14.

[24] Arulampalam MS, Maskell S, Gordon N, Clapp T. A tutorial on particle filters for online nonlinear/non-Gaussian Bayesian tracking. Signal Processing, IEEE Transactions on 2002;50:174–88.

[25] Doucet A, Godsill S, Andrieu C. On Sequential Monte Carlo Sampling Methods for Bayesian Filtering. Statistics and Computing 2000;10:197–208.

[26] Cappé O, Godsill SJ, Moulines E. An overview of existing methods and recent advances in sequential Monte Carlo. Proceedings of the IEEE 2007;95:899–924.

[27] Orchard ME, Vachtsevanos GJ. A particle-filtering approach for on-line fault diagnosis and failure prognosis. Transactions of the Institute of Measurement and Control 2009;31:221–46.

[28] Baraldi P, Cadini F, Mangili F, Zio E. Model-based and data-driven prognostics under different available information. Probabilistic Engineering Mechanics 2013;32:66–79.

[29] Tulsyan A, Huang B, Bhushan Gopaluni R, Fraser Forbes J. On simultaneous on-line state and parameter estimation in non-linear state-space models. Journal of Process Control 2013;23:516–26.

[30] Chen T, Morris J, Martin E. Particle filters for state and parameter estimation in batch processes. Journal of Process Control 2005;15:665–73.

[31] Liu J, West M. Combined parameter and state estimation in simulation-based filtering. Springer; 2001.

[32] Wan-ping W, Sheng L, Ting-wen X. Particle filter for state and parameter estimation in passive ranging. Intelligent Computing and Intelligent Systems, 2009. ICIS 2009. IEEE International Conference on, vol. 3, IEEE; 2009, p. 257–61.

[33] Roemer MJ, Kacprzynski GJ. Advanced diagnostics and prognostics for gas turbine engine risk assessment. Aerospace Conference Proceedings, 2000 IEEE 2000;6:345–53 vol.6.

[34] Baraldi P, Mangili F, Zio E. Ensemble of bootstrapped models for the prediction of the remaining useful life of a creeping turbine blade. Prognostics and Health Management (PHM), 2012 IEEE Conference on 2012:1–8.

[35] Marahleh G, Kheder ARI, Hamad HF. Creep life prediction of service-exposed turbine blades. Materials Science and Engineering: A 2006;433:305–9.

[36] Carter TJ. Common failures in gas turbine blades. Engineering Failure Analysis 2005;12:237–47.

[37] Chaboche JL. Anisotropic creep damage in the framework of continuum damage mechanics. Nuclear Engineering and Design 1984;79:309–19.

[38] Saanouni K, Chaboche JL, Bathias C. On the creep crack growth prediction by a local approach. Engineering Fracture Mechanics 1986;25:677–91.

[39] Swindeman RW, Swindeman MJ. A comparison of creep models for nickel base alloys for advanced energy systems. International Journal of Pressure Vessels and Piping 2008;85:72–9.

[40] Baraldi P, Mangili F, Zio E. Investigation of uncertainty treatment capability of model-based and data-driven prognostic methods using simulated data. Reliability Engineering & System Safety 2013;112:94–108.

[41] Sinn H-W. A REHABILITATION OF THE PRINCIPLE OF INSUFFICIENT REASON. Quarterly Journal of Economics 1980;94:493–506.

APPENDIX 1: PF-OTKS FOR CASE 1

The key problem in PF-OTKS is to define the "updating" distribution of the parameters $p(\mathbf{P}_t|\mathbf{P}_{t-1})$. Unlike for the distribution of the degradation state $p(\mathbf{x}_t|\mathbf{x}_{t-1})$, there is no direct definition for $p(\mathbf{P}_t|\mathbf{P}_{t-1})$ because there is not an equation describing the parameters evolution process, analogous to the state equation (2.3).

The common ways to proceed are to keep $\mathbf{P}_t$ unchanged (equation (6.1) below) or add a Gaussian noise on $\mathbf{P}_t$ (equation (6.2) below):

$$\mathbf{p}_{t+1}^{i} = \mathbf{p}_t^{i} \tag{6.1}$$

$$\mathbf{p}_{t+1}^{i} = \mathbf{p}_t^{i} + N(0, \sigma_{AN}^2) \tag{6.2}$$

However, both these two ways tend to the problem of particle impoverishment in PF and render convergence difficult to achieve (the variance of the posterior distribution is large) [10]. The OTKS method can be used to handle $p(\mathbf{P}_t|\mathbf{P}_{t-1})$ and solve these problems [11].

OTKS applies two procedures to the population of particles: shrinkage and perturbation. Shrinkage aims at concentrating the particles to their estimated values, whereas perturbation adds a controlled noise to the particles in order to maintain the diversity of the particle population.

The shrinkage is performed by:

$$\tilde{\mathbf{P}}_t^{i} = \mathbf{P}_t^{i}\sqrt{1-h^2} + \hat{\mathbf{P}}_t\left(1-\sqrt{1-h^2}\right) \tag{6.3}$$

where $\tilde{\mathbf{P}}_t^{i}$ is the *i*-th particle after the shrinkage. The smoothing parameter, $h \in [0,1]$, determines the degree of shrinkage: higher value of h means more shrinkage of the particles to the estimated values. If $h = 1$, the particles completely shrink to $\hat{\mathbf{P}}_t$; whereas if $h = 0$, no shrinkage is taken. After shrinkage, the variance in the population of particles decreases to $(1-h^2)V(\mathbf{P}_t^{i})$. Then, $\tilde{\mathbf{P}}_t^{i}$ can be used as the input of $p(\mathbf{x}_{t+1}|\mathbf{x}_t, \tilde{\mathbf{P}}_t^{i})$ to predict the x_{t+1}^{i}, based on the equation (2.3):

$$x_{t+1}^{i} = f_0\left(x_t^{i}, \tilde{\mathbf{P}}_t^{i}, t, \omega_t\right) \cdot g\left(e_t, t, \omega_t\right) \tag{6.4}$$

Perturbation is used to compensate the particles variance, by adding a Gaussian noise with variance $h^2V(\mathbf{P}_t^{i})$ to the *i*-th particle at the next time step:

$$\mathbf{P}_{t+1}^{i} = \tilde{\mathbf{P}}_t^{i} + N\left(0, h^2V\left(\mathbf{P}_t^{i}\right)\right) \tag{6.5}$$

In this way, the variance of $\mathbf{P}_t^{i}$ remains unchanged after the kernel smoothing, namely $V(\mathbf{P}_{t+1}^{i}) = V(\mathbf{P}_t^{i})$, while diversity is still injected in the particle population.

The value of the smoothing parameter *h* is very important for the performance of kernel smoothing. Some researchers suggest using a constant *h* or adjust it based on historical data on similar components [28, 30]. Since these data are unavailable in our work, the only information that can be used to set *h* is the measurements of degradation state collected on-line along the developing degradation trajectory.

In [29], the authors propose to adjust the value of h according to the newest collected on-line measurement. The key issue is to find the value of h which projects the predicted distribution (given by $p(\mathbf{x}_t|\mathbf{x}_{t-1}, \mathbf{P}_{t-1})$ into the high density area of the posterior distribution (given by $p_e(\mathbf{x}_t|z_{1:t})$). This is achieved by seeking the minimum Kullback–Leibler (KL) divergence between $p(\mathbf{x}_t|\mathbf{x}_{t-1}, \mathbf{P}_{t-1})$ and $p_e(\mathbf{P}_t|z_{1:t})$. In the framework of PF, this KL divergence can be calculated as:

$$KL(h_t) = -\sum_{i=1}^{N} w_{t-1}^i \log\left(w_t^i\right) \tag{6.6}$$

where $KL(h_t)$ is the KL divergence given the smoothing parameter h_t. The optimal smoothing parameter h_t^* is obtained by minimizing $KL(h_t)$:

$$h_t^* = \arg\min_{h_t \in [0,1]} \left[KL(h_t) \right] \tag{6.7}$$

Finally, by substituting h_t^* into equation (6.3), one obtains a new equation for the particle shrinkage:

$$\tilde{\mathbf{P}}_t^i = \mathbf{P}_t^i \sqrt{1-\left(h_{t+1}^*\right)^2} + \hat{\mathbf{P}}_t \left(1-\sqrt{1-\left(h_{t+1}^*\right)^2}\right) \tag{6.8}$$

Notice that the execution of the shrinkage at time t requires h_{t+1}^*, which needs the information of on-line measurement $\boldsymbol{z}_{t+1}$ at time t+1. The details of the procedures of OTKS can be found in [11]. The pseudocode for PF-OTKS can be written as follows:

Sample $x_0^i \sim p(x_0), \mathbf{P}_0^i \sim p(\mathbf{P}_0)$, set initial weight $w_0^i = N^{-1}, i = 1, 2, ..., N$

t=1;

While (t<T_end)

Get the new measurement z_t, calculate the optimal h_t^* value using equations (6.6) and (6.7);

Shrink $\mathbf{P}_{t-1}^i$ using equation (6.8) with h_t^*, and get $\tilde{\mathbf{p}}_{t-1}^i$;

Calculate the predicted particle x_t^i with $\tilde{\mathbf{p}}_{t-1}^i$ using equation (6.4);

Perform the perturbation on $\tilde{\mathbf{p}}_{t-1}^i$ using equation (6.5) and get $\mathbf{P}_t^i$;

Calculate the weight $w_t^i = w_{t-1}^i \, p(z_t \mid x_t^i) \Big/ \sum_{i=1}^{n} p(z_t \mid x_t^i)$ using equation (3.2);

Calculate the posterior PDF and expectation of the degradation state and parameters, $p_e(x_t|z_{1:t}), p_e(\mathbf{P}_t|z_{1:t}), \hat{x}_t$ and $\hat{\mathbf{P}}_t$, using equation (3.1);

Calculate the Effective Sample Size (ESS) criterion for resampling: $ESS_t \approx \left(\sum_{i=1}^{n} \left(w_t^i\right)^2 \right)^{-1}$;

if $ESS_t \le N/2$

resample with probability $\mathrm{P}(x_t^i = x_{t-1}^i) = w_{t-1}^i, \mathrm{P}(\mathbf{P}_t^i = \mathbf{P}_{t-1}^i) = w_{t-1}^i$;

end if

t=t+1;
end while

APPENDIX 2: PF-OTKS FOR CASE 2

Using PF-OTKS described in subsection 2.1.1, we can estimate the PDF of $\mathbf{L}_t$. The particles of x_{t+1} can be calculated as:

$$x_{t+1}^i = f_0\left(x_t^i, \mathbf{P}_t^i, t, \omega_t\right) \cdot U_t^i,\ U_t^i \sim Y\left(\mathbf{L}_t^i\right) \tag{6.9}$$

The pseudocode for PF-OTKS in case 2 can be written as follows:

Sample $x_0^i \sim p(x_0), \mathbf{L}_0^i \sim p(\mathbf{L}_0)$, set initial weight $w_0^i = N^{-1}, i = 1, 2, ..., N$

t=1;

While (*t*<T_end)

Get the new measurement z_t, calculate the optimal h_t^* value using equations **(6.6)** and **(6.7)**;

Shrink $\mathbf{L}_{t-1}^i$ with h_t^* using equation **(6.8)**, and get $\tilde{\mathbf{L}}_{t-1}^i$;

Calculate the predicted particle x_t^i with $\tilde{\mathbf{L}}_{t-1}^i$ using equation (6.9);

Perform the perturbation on $\tilde{\mathbf{L}}_{t-1}^i$ using equation **(6.5)** and get $\mathbf{L}_t^i$;

Calculate the weight $w_t^i = w_{t-1}^i \, p(z_t \mid x_t^i) \Big/ \sum_{i=1}^{n} p(z_t \mid x_t^i)$ using equation (3.2);

Calculate the posterior PDF and expectation of the degradation state and parameters, $p_e(x_t \mid z_{1:t}), p_e(\mathbf{P}_t \mid z_{1:t}), \hat{x}_t$ and $\hat{\mathbf{P}}_t$, using equation (3.1);

Calculate the Effective Sample Size (ESS) criterion for resampling: $ESS_t \approx \left(\sum_{i=1}^{n} \left(w_t^i \right)^2 \right)^{-1}$;

if $ESS_t \le N/2$

resample with probability $\mathrm{P}(x_t^i = x_{t-1}^i) = w_{t-1}^i, \mathrm{P}(\mathbf{L}_t^i = \mathbf{L}_{t-1}^i) = w_{t-1}^i$;

end if

t=t+1;

end while

Figures:

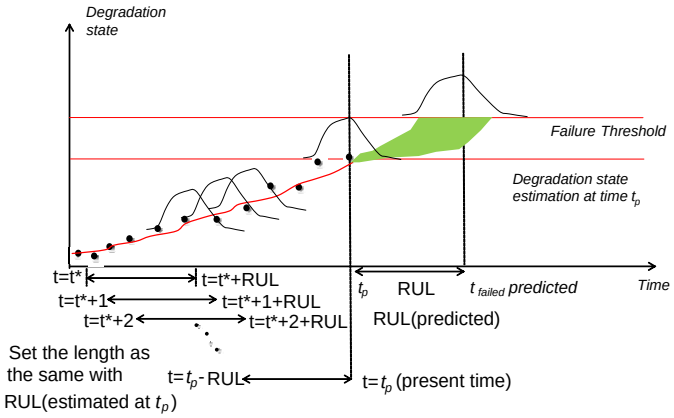

Figure 1 Sketch of moving time window approach

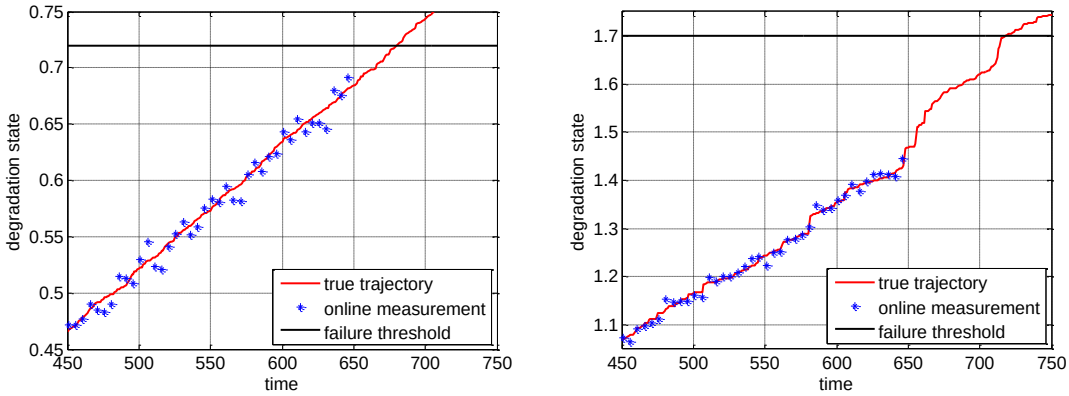

Figure 2. Two examples of simulated degradation trajectories in the small (left) and large (right) uncertainty settings of the process noise.

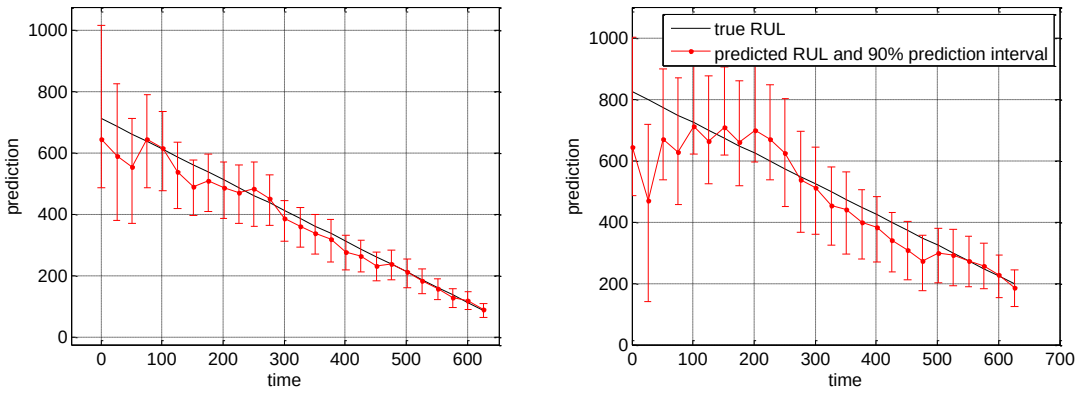

Figure 3 RUL prediction in Case 1.
Left: small uncertainty on the blade stress; right: large uncertainty on the blade stress

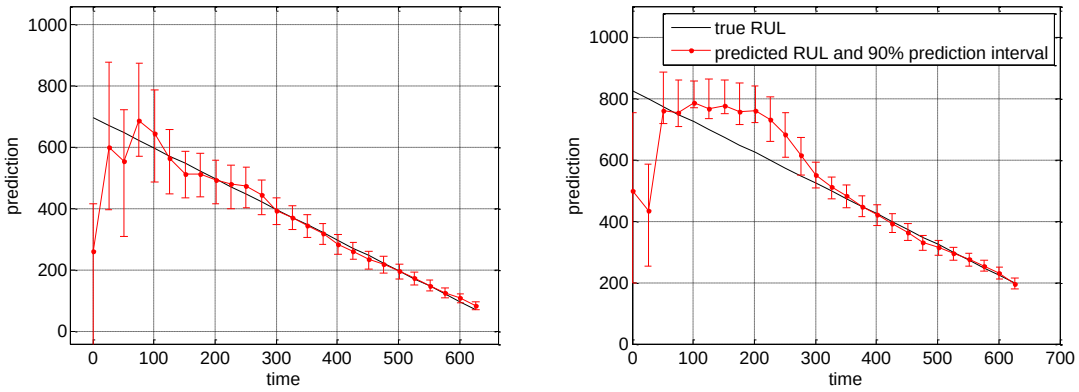

Figure 4 RUL prediction in Case 2.
Left: small uncertainty on the blade stress; right: large uncertainty on the blade stress

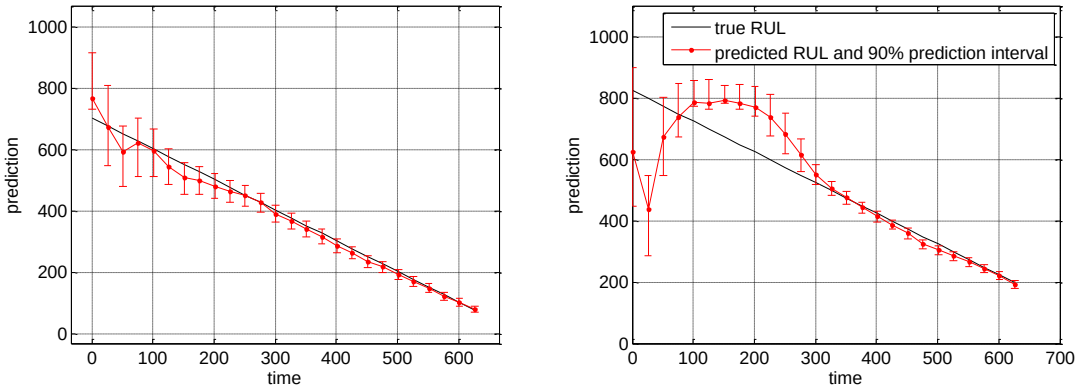

Figure 5 RUL prediction in Case 3.
Left: small uncertainty on the blade stress; right: large uncertainty on the blade stress

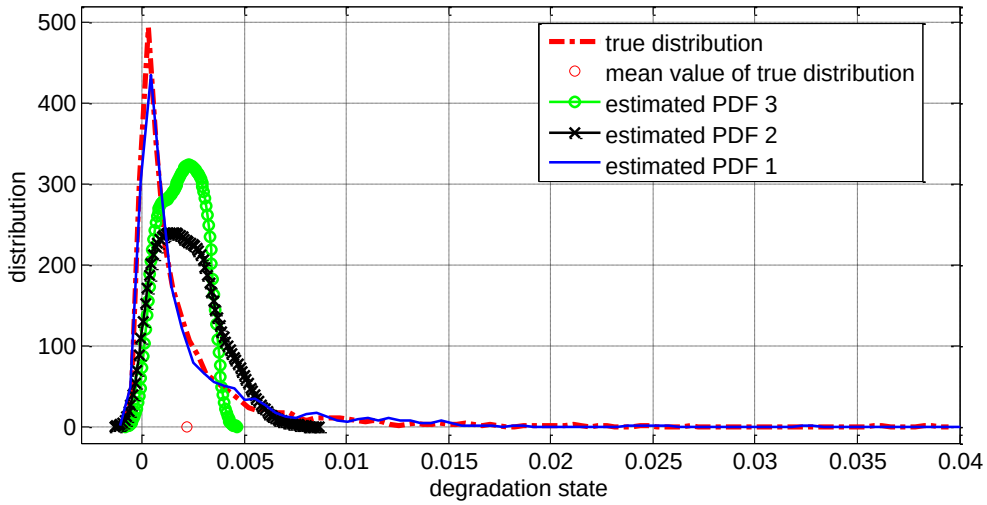

Figure 6 Probability Distribution Functions (PDFs) of degradation rate

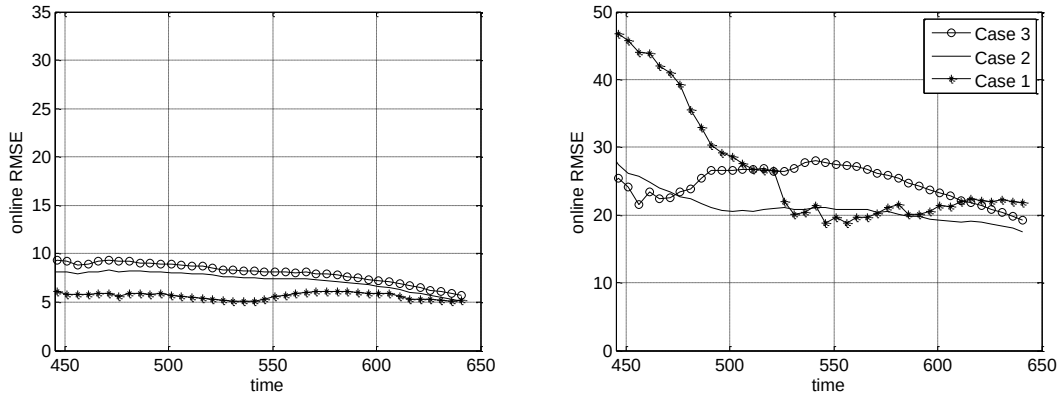

Figure 7 On-line RMSE.
Left: small uncertainty on the blade stress; right: large uncertainty on the blade stress

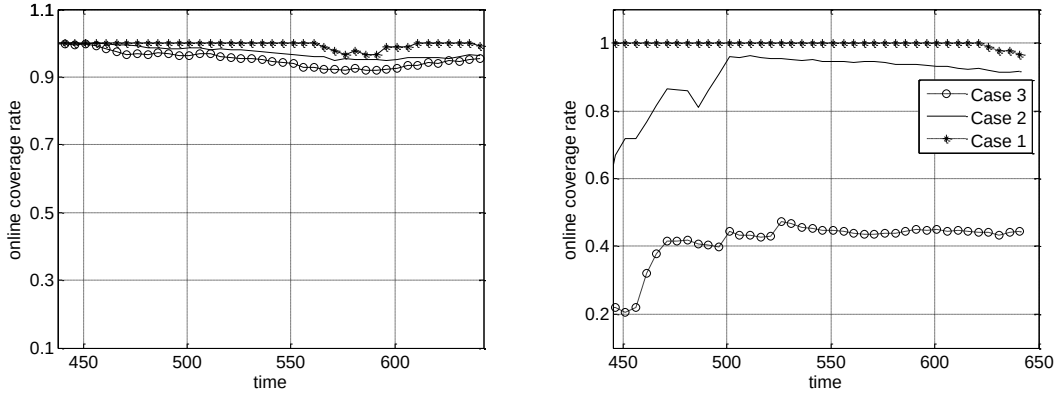

Figure 8 On-line CR.
Left: small uncertainty on the blade stress; right: large uncertainty on the blade stress

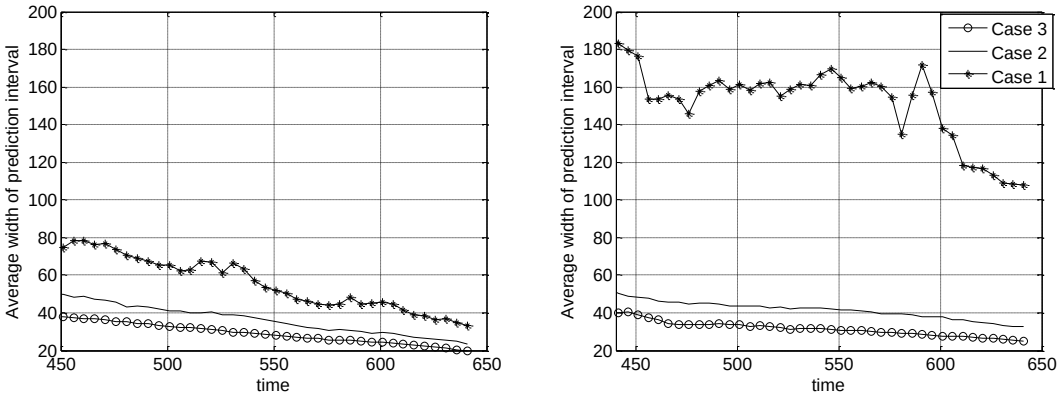

Figure 9 On-line average width of prediction interval.
Left: small uncertainty on the blade stress; right: large uncertainty on the blade stress

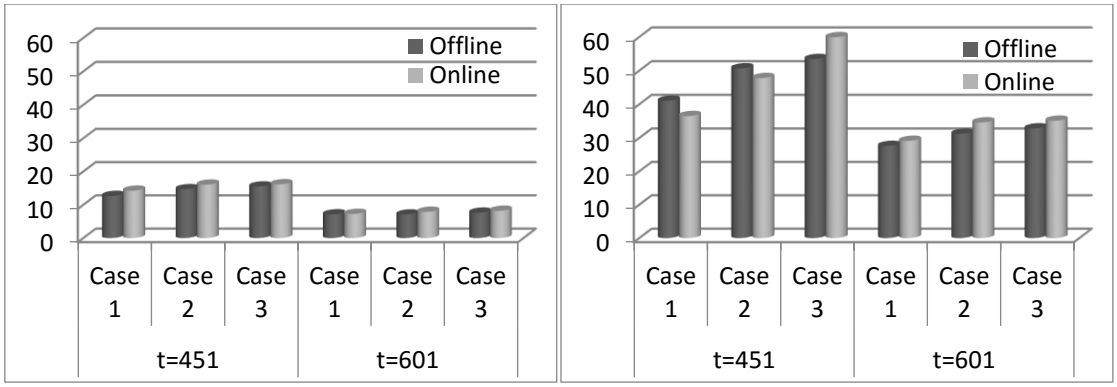

Figure 10 On-line and off-line RMSE
Left: small uncertainty on the blade stress; right: large uncertainty on the blade stress

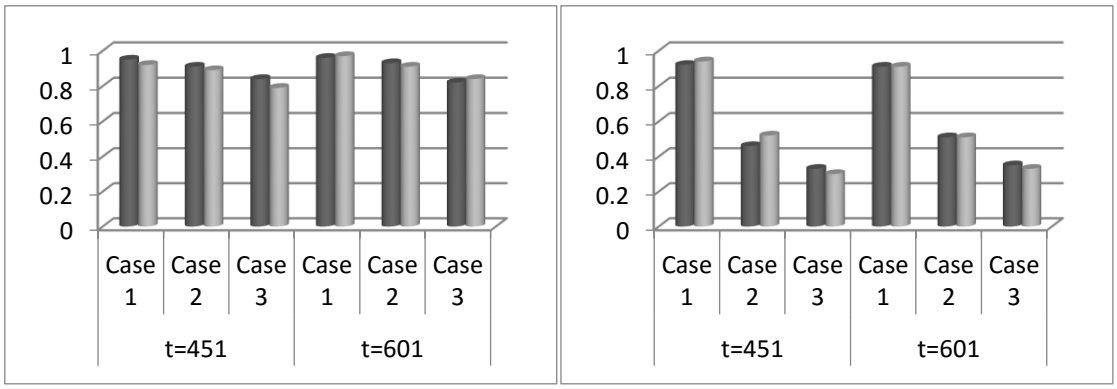

Figure 11 On-line and off-line CR.
Left: small uncertainty on the blade stress; right: large uncertainty on the blade stress

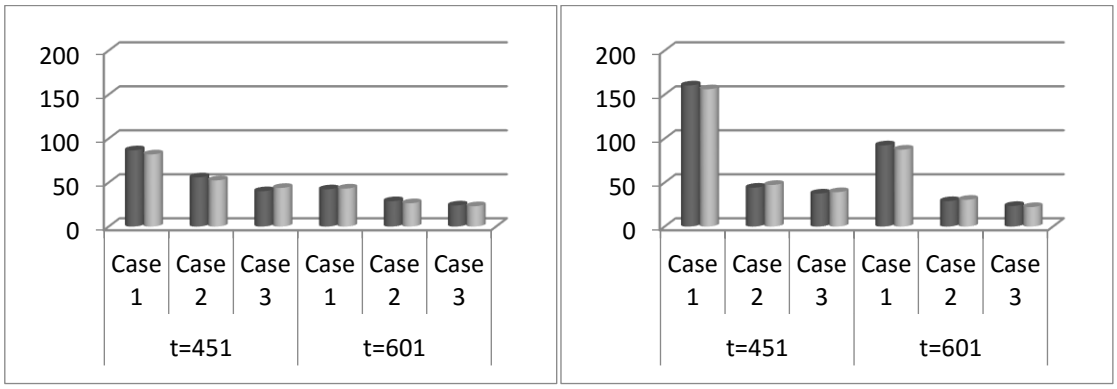

Figure 12 On-line and off-line average width of prediction interval.
Left: small uncertainty on the blade stress; right: large uncertainty on the blade stress

Tables:

Table 1 Time window attributes

Time Window win_t attribute	value
start time	t
end time	$t + R\hat{U}L_{t_p}$
Best estimation of the degradation state PDF at $t + R\hat{U}L_{t_p}$ based on the measurements collected until the present time t_p	$p_e\left(x_{t+R\hat{U}L_{t_p}} \middle\| z_{1:t_p}\right)$
Predicted PDF of the degradation state at time $t + R\hat{U}L_{t_p}$ based on the measurements collected until time t	$p_f\left(x_{t+R\hat{U}L_{t_p}} \middle\| z_{1:t}\right)$
Assumed failure threshold	$\hat{x}_{t+R\hat{U}L_{t_p}\|z_{1:t_p}}$
Predicted PDF of RUL at time t	$p_f(RUL_t \| z_{1:t}, Th_t)$
True RUL at time t	$R\hat{U}L_{t_p}$

Table 2 Parameters of the degradation model

Physical parameters	
A	6.9e-3 $(N/m^2)^{-n}/day$
n	6.01
Q	2.9e5 J/mol
R	8.31
K	1.1e-3 Kg/m
Δt	5 days

Table 3 Parameters of the distributions representing the process noises

	Small uncertainty on the blade stress	**Large uncertainty on the blade stress**
ω_t	N(3000,30)	N(3000,30)
T_t	N(1100,11)	N(1100,11)
γ_t	***N*(0,10)**	***N*(0,30)**
Th	0.72	1.7

Table 4 Prior distributions of the uncertain parameters

	Case 1	Case 2	Case 3
$N_s = 10$ (small uncertainty on the blade stress)	A~ U (5.5e-4, 1.05e-2) n~ U (5.5, 6.1)	L_t ~ U (8e10,1.2e11) H_t ~ U (1.6e12, 2.2e13)	L_t' ~ U (5e-6, 1.2e-5) H_t' ~ U (1.5e-4, 5.5e-4)
$N_s = 30$ (large uncertainty on the blade stress)	A~ U (5.5e-4, 1.05e-2) n~ U (5.5, 6.1)	L_t ~ U (4e10, 8e10) H_t ~ U (1.2e12, 2.2e13)	L_t' ~ U (5e-6, 1.5e-5) H_t' ~ U (2e-4, 2e-3)